VIII International Conference on Computational Methods in Marine Engineering
MARINE 2019
R. Bensow and J. Ringsberg (Eds)

Experimental validation of aerodynamic computational results in the aft-deck of a simplified frigate shape (SFS2)

MARINE 2019

R. BARDERA†, J.C. MATIAS*, A. GARCIA-MAGARIÑO†

Instituto Nacional de Técnica Aeroespacial (INTA)
Ctra. Ajalvir, km 4.5
Torrejón de Ardoz, 28850 Madrid, Spain

†e-mail: barderar@inta.es, web page: http://www.inta.es
*e-mail: matiasgjc@inta.es, web page: http://www.inta.es
†e-mail: garciamga@inta.es, web page: http://www.inta.es

Key words: aerodynamics, frigate, helicopter, flight-deck, wind-tunnel, CFD validation, PIV.

Abstract. Military frigates develop an essential tactical element and have a great importance in all navies operations around the world since they provide marine and submarine surveillance, as well as support for different emergencies, rescue, and humanitarian aid. These operations increase their range, even more, when the frigate allows for helicopter operations on its deck. Thus, troops can be transported between frigates and surveillance and rescue operations can be done faster. However, the aerodynamic interference between frigate and helicopter results in a complex airflow which causes an increase in the pilot's workload during aircraft operations above the helideck. This complex airflow is due to the fact that the frigate has a non-aerodynamic design with sharp surfaces. They cause large areas of turbulent detached flow and low-velocity recirculation zones above the flight deck endangering helicopter take-off and landing maneuvers. For this reason, a large number of tests must be carried out on all frigates which can host helicopters operations. Tests have traditionally been performed in wind tunnels. Advances in the computing power of computers and their costs reduction have allowed better *computational fluid dynamics* (CFD) analysis reducing the need for experimental testing. However, CFD still has certain problems in predicting some complex flows such as the perturbed flow over the flight deck located in the wake of a frigate resulting in a necessity of validation by experimental data. The aim of this paper is to conduct a comparative study between numerical and experimental results of the flow around a *simplified frigate shape* (SFS2). The numerical study has been performed using a commercial software (FLUENT). The experimental study has been carried out in *Instituto Nacional de Técnica Aeroespacial* INTA (Spain) by wind tunnel testing a sub-scaled SFS2 model by means of *Particle Image Velocimetry* (PIV). The assessment is made by comparing point by point the velocity values obtained from experimental maps with those obtained in the numerical study. The comparison focuses on the helicopter rotor plane during its approach to the frigate. All the results presented could be a step forward in solving computational problems and improve their results related to marine engineering. They also could provide an important basis as a powerful validation method for future researches.

1. INTRODUCTION

Helicopters are currently a very useful operational tool for military operations on frigates. They make it possible to support anti-submarine and surface warfare, surveillance tasks, or even to transfer troops between different frigates [1]. For this reason, helicopters operation in frigates is presented as an essential element among modern naval operations.

In general, a frigate superstructure is essentially a combination of non-aerodynamic bodies that generate a very complex flow around them, affecting the helicopter operations on the ship [2-4]. This makes take-off and landing operations at its deck difficult and in certain circumstances risky. The most common position for the helicopter platform on a frigate is at the stern. It is a point where the ship's superstructure generates a large recirculation bubble caused by the detachment of the flow [5-7]. This flow structure, in contrast to the free stream wind velocity experienced by the helicopter during the approach procedure to the frigate, is what causes oscillations and low-frequency movements on the helicopter, increasing pilot workload during the maneuver [8-13].

The aim of this paper is to obtain velocity maps above the helideck of a "Simplified Frigate Shape" (SFS2) by means of numerical results and Particle Image Velocimetry (PIV) in wind tunnel tests. Thus, the flow structure, which affects the helicopter rotor during the landing maneuver of a helicopter, will be analyzed and the differences founded in the results using numerical and experimental methods will be compared.

2. HELICOPTER LANDING MANEUVER ON FRIGATES

All navies have standardized procedures related to aircraft operations on military ships. The case of the helicopter landing on decks is not an exception, and one of the most common maneuvers is the fore/aft approach [14]. This maneuver is performed in three steps, as can be seen in *figure 1*.

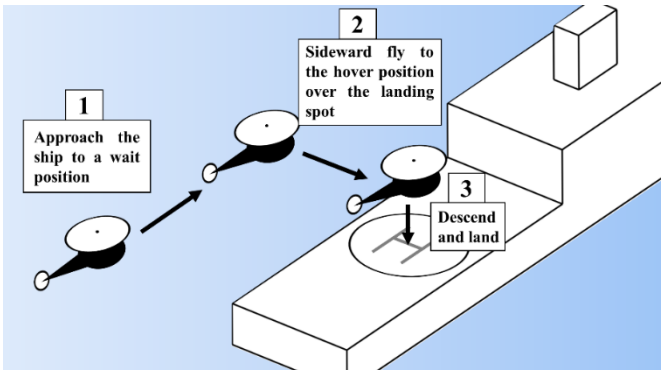

Figure 1: Diagram of the procedure for aft landing on a frigate.

For the tests, a distance equal to the beam of the frigate will be taken for the helicopter waiting point on the port side of the frigate (point 2 in *figure 1*). In this way, the sideward displacement flies half over the water and half over the deck.

3. NUMERICAL STUDY SETUP

In this section, the process followed to get numerical results of the flow around a simplified frigate model is explained.

3.1. Simplified frigate model geometry

Figure 2 (left) shows the dimensions of the frigate model used for the tests. It is a simplified frigate model proposed by NATO, on a scale of 1:85, called SFS2 ("*Simplified Frigate Shape*"). Its shape represent the part of the frigate above the waterline i.e. the superstructure and exhaust gases stack by means of simple prismatic blocks, which imitate the poorly aerodynamic geometries presents in conventional frigates. This model has been widely used for aerodynamic research. Its simplicity allows easy numerical implementation or simple manufacturing for experimental tests. [15-17].

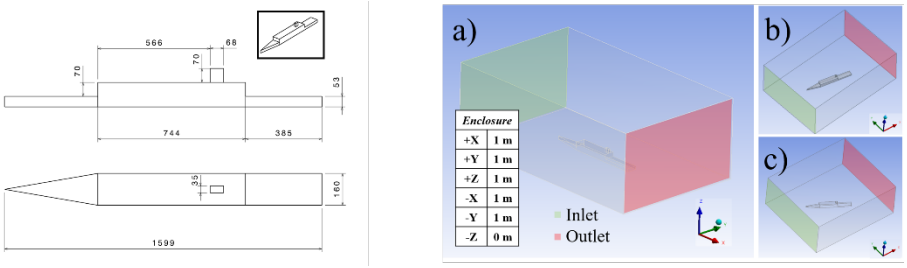

Figure 2: At the left, 1:85 SFS2 dimensions (mm). At the right, control volume of the problem in the ANSYS Design Modeler for $WOD = 0º$ (a), 15º (b) and 30º cases (c).

For the numerical study, the model was created as a 3D virtual model using CATIA V5 software. The model was imported in .igs format to the Design Modeler program available in ANSYS Workbench. The Design Modeler allows creating a contour around the full body using the enclosure function. The contour dimensions selected for this study were $-z = 0\ m$ (representing the sea level surface) and 1 m in all directions, measured from the surface of the body, *figure 2a*. Finally, a boolean operation was made to the body and the contour created to define the control volume of the fluid.

As both experimental and numerical studies were made in three different inlet configurations (*Wind Over Deck angle*, $WOD = 0º$, 15º and 30º), three different control volumes were created with the model turned, *figure 2 (right), 2a, 2b, 2c*.

3.2. Mesh generation

Once the model geometry and the control volume is defined, the next step is to generate the mesh. Using the *Mesh Generator* from ANSYS Workbench and limiting the tetrahedral elements size to a maximum of $4 \times 10^{-2}\ m$, a 475K cells mesh was created. It was under the FLUENT Student limit of 512K elements and it allowed to obtain results considerably quickly. Mesh refinements were made to improve results quality close to the body. Finally, *Named selections* were created for the *inlet* and *outlet* surfaces to help the solver to boundary conditions definition. *Figure 3* shows the mesh generated for the control volumes created.

Figure 3: Mesh generated for 0º, 15º and 30º (a, b, c) cases in ANSYS Mesh Generator.

3.3. Solver settings

The software used to get the fluid mechanics results was FLUENT. The program was adjusted for calculating the results using four processors working in parallel with a dedicated GPU. The energy equation was disabled and the k-epsilon Realizable viscous model with standard wall functions was used. The boundary conditions were similar for the three cases studied: a constant velocity magnitude of 10 m/s at the inlet and a null gauge pressure at the outlet ($P_{out} = P_{ambient}$). Both inlet and outlet were adjusted with a turbulence intensity of 10 % and a turbulence length scale of 0.16 m, based on the width of the scaled model.

The calculation methods selected for the turbulent kinetic and dissipation rate were first order upwind schemes in a first attempt. For the final and more accurate results, a second order was used. A standard initialization computed from the inlet surface data was used. Finally, a limit of 3.000 iterations was imposed. However, the real number of iterations enough to get the solution convergence were less than 200 in the three cases.

3.4. Exporting results

The first step to get the numerical results of each case was to create contours from plane surfaces. The contours can present different magnitudes of interest such as pressures, velocities, turbulence or vorticity. *Figure 4* presents the velocity contours obtained for the 0º of inlet velocity case in two different planes: the symmetry plane and the rotor plane. The symmetry plane is a vertical plane created from the center line of the frigate. The rotor plane is a horizontal plane located at a height in which the rotor is working during the helicopter approach (5 m above the deck at the real case, 58 mm scaled).

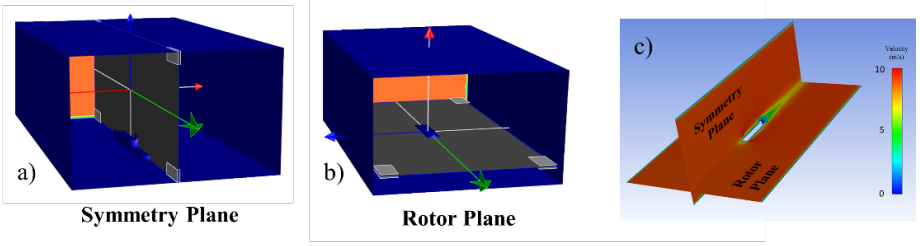

Figure 4: Symmetry (a) and rotor (b) planes defined in the control volume. Velocity contours of symmetry and rotor plane for 0º case (c).

All data contained on the rotor plane, which contains the results that are the objective of this study, was exported as an ASCII file in order to be able to make calculations using these results. For example to make velocity values non-dimensional or to get a specific point value through interpolation to compare with experimental data (see *section 5.3: comparison*).

4. EXPERIMENTAL SETUP

4.1. Wind tunnel

In order to experimentally characterize the flow over the flight deck of the frigate, experimental tests were carried out in wind tunnel T1 at the Instituto Nacional de Técnica Aeroespacial (INTA), Spain. This wind tunnel has a closed circuit with an open test section (3 × 2 m^2). In the test section a maximum flow velocity up to 60 m/s with a turbulence intensity under 0.5 % can be reached.

4.2. Simplified frigate model

The same model presented in *figure 2* was made of wood for wind tunnel testing. For the tests, due to the fact that the PIV laser plane available in the wind tunnel is vertical, and horizontal velocity maps are desired, the model was fixed to a vertical wall as can be seen in *figure 5*. In addition, a bolt was used to fix the model to the wall at the proper wind incidence angle (WOD which means *Wind Over Deck* angle). As the helicopter maneuver must be carried out at 5 meters height above the deck, the planes were taken at a distance of 58 mm from the deck of the model (scale 1:85).

All tests were performed at 10 m/s, which results in a Reynolds number based on the beam of the frigate of 1.09×10^5. This value is above the critical value that is necessary to satisfy the laws of dynamic similarity between the flow on the model and on the real frigate [18].

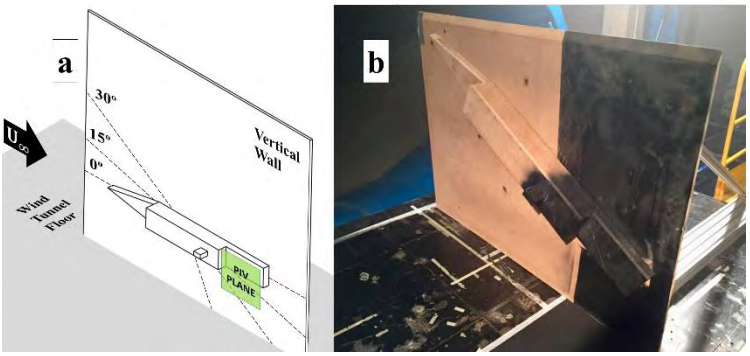

Figure 5: a) Positioning diagram of the frigate and the velocity measuring plane PIV b) Frigate model SFS2 placed in the wind tunnel test chamber at WOD = 30º.

4.3. Particle Image Velocimetry

Particle Image Velocimetry (PIV) was used for the experimental tests. It is an advanced and non-intrusive velocity measurement technique that needs an airflow seeded with small tracer particles which are illuminated by means of a laser plane in order to capture them in two pictures, separated a short time Δt [19-22]. Thus, by making a correlation between the pair of images captured, it is possible to measure the displacement of the particles (ΔX). As the time between captures (Δt) is known, it is possible to obtain the local speed $\bar{u}$ with the following expression contained *in figure 6*,

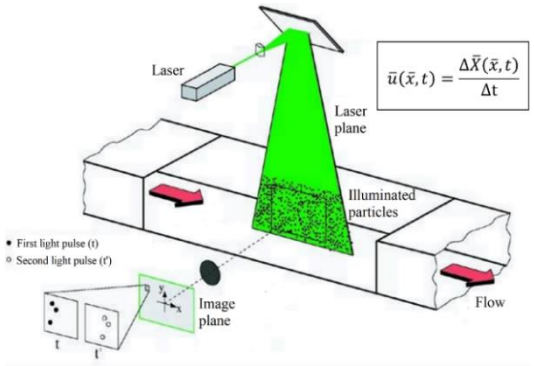

Figure 6: Operating diagram of PIV system

The required equipment for this technique consisted of a particle generator, a laser light source, an image recording system, a synchronizer and a processor system. Laskin atomizers were used as particle generators, which allow the production of very small particles ($\sim 1\ \mu m$) that are able to acquire quickly the local velocity of the flow [23, 24]. The laser light source consists of two Nd:YAG pulsed lasers (Neodymium: Yttrium Aluminium Garnet). To capture the images, a digital camera was used, which consisted of a CCD sensor of 2048 × 2048 pixels and a lens that allows regulating the entry of light and focus. A synchronizer is required to trigger the lasers at the appropriate time and synchronize them with the captures taken by the camera. Finally, a processing system must correlate the small interest windows of 32 × 32 pixels of each pair of images taken, to obtain the particle displacement and then their velocity. After this correlation, the velocity maps can be obtained. *Figure 6* shows the simplified scheme of operation of the PIV system.

5. RESULTS

5.1. Numerical results

Figure 7 shows the non-dimensional velocity maps of the rotor plane locations obtained directly from FLUENT results. Dashed black squares represent the interest windows in which the experimental and numerical comparison will be focused.

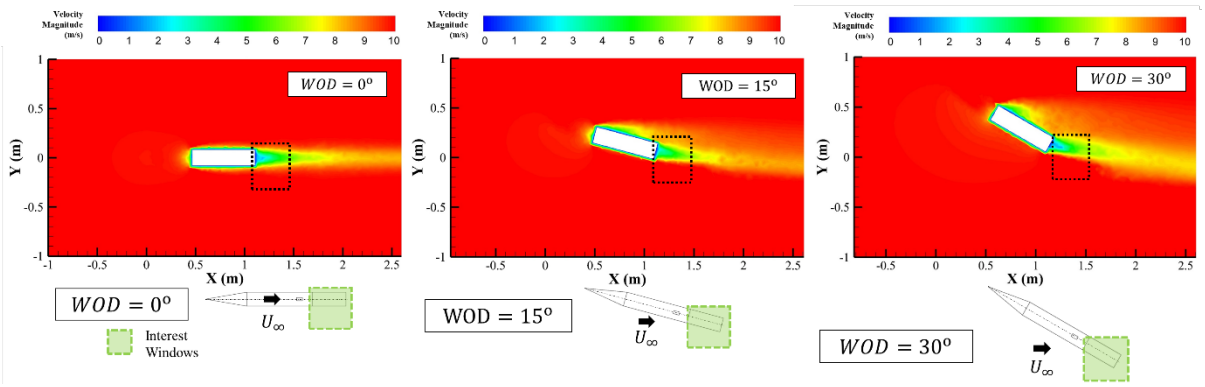

Figure 7: Numerical results of Velocity maps at 0º, 15º and 30º

In all of three cases presented, it can be observed an airflow wake with a huge recirculation region of the flow, caused by the presence of the frigate superstructure. This flow structure could negatively affect the helicopter approach operation to the frigate.

5.2. Experimental results

Figure 8 shows the PIV non-dimensional velocity maps for $WOD = 0^o,\ 5^o, 30^o$ obtained from experimental tests performed. All of them were captured at the same 58 mm above the frigate flight deck. The black line in the maps represents the helicopter trajectory during the landing maneuver towards the helideck at the stern described in *section 2*. Dashed red lines indicate the area of the rotor occupied during helicopter landing procedure.

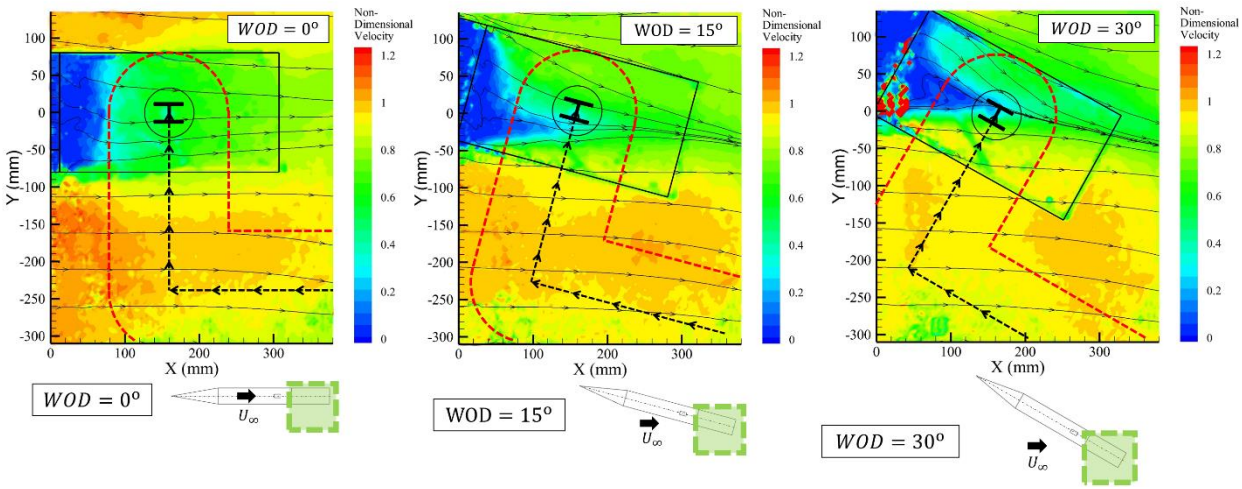

Figure 8: PIV non-dimensional velocity maps at WOD = 0º, 15º and 30º. Landing path of the helicopter marked in black lines.

As can be observed at the previous maps, in all three cases there is a low-velocity area caused by the detachment of the airflow caused by the frigate superstructure ($x \sim 50\ mm$; $y \sim 0\ mm$). This is a typical path of a flow, which is immediately behind from a descending step. For the helicopter landing procedure, it is clearly visible that although most of the maneuver is immersed to clean airflow condition, in the last phase of the approach when the helicopter moves laterally towards the point of descent, its rotor experiences a large change in incident velocities, caused by the presence of the frigate superstructure.

5.3. Comparison

As the same velocity maps have been obtained by experimental and numerical methods, they can be compared. However, the coordinates of the points in which the values are known on both tests do not exactly match. The experimental maps points are distributed according to the interest windows size of PIV (32 × 32 pixels), while in the numerical results, each point associated with a value coincides with the mesh nodes. This problem has been solved by interpolating the numerical results in the same coordinates of the experimental results as shown in *figure 9*. In this figure, V_{CFD_i} are the velocities obtained by numerical results, h_i are the distances between each point i and the desired CFD_PIV, and V_{CFD_PIV} is the desired interpolated velocity at the same point where the PIV velocity is already known.

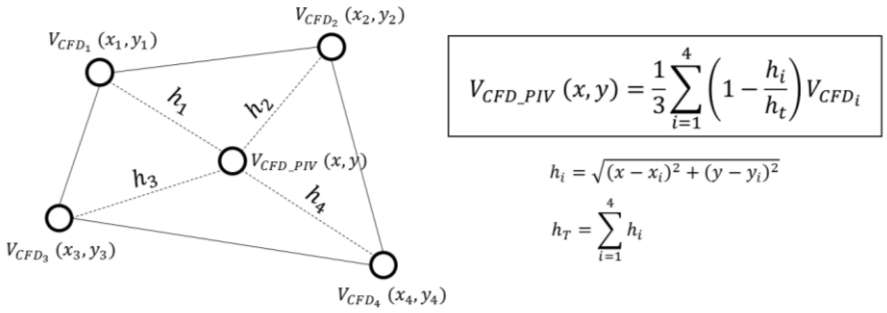

Figure 9: Interpolation to get CFD velocity values at experimental PIV coordinates.

Applying the above formula to the numerical results and representing the values in similar maps than PIV results, CFD Velocity maps in *figure 10* are obtained. Results presented show a big resemblance of the main flow patterns and velocity values over the aft-deck using both methods. In all maps, the helicopter trajectory is represented with black arrowed lines and the volume occupied by the rotor position during the maneuver with dashed red lines.

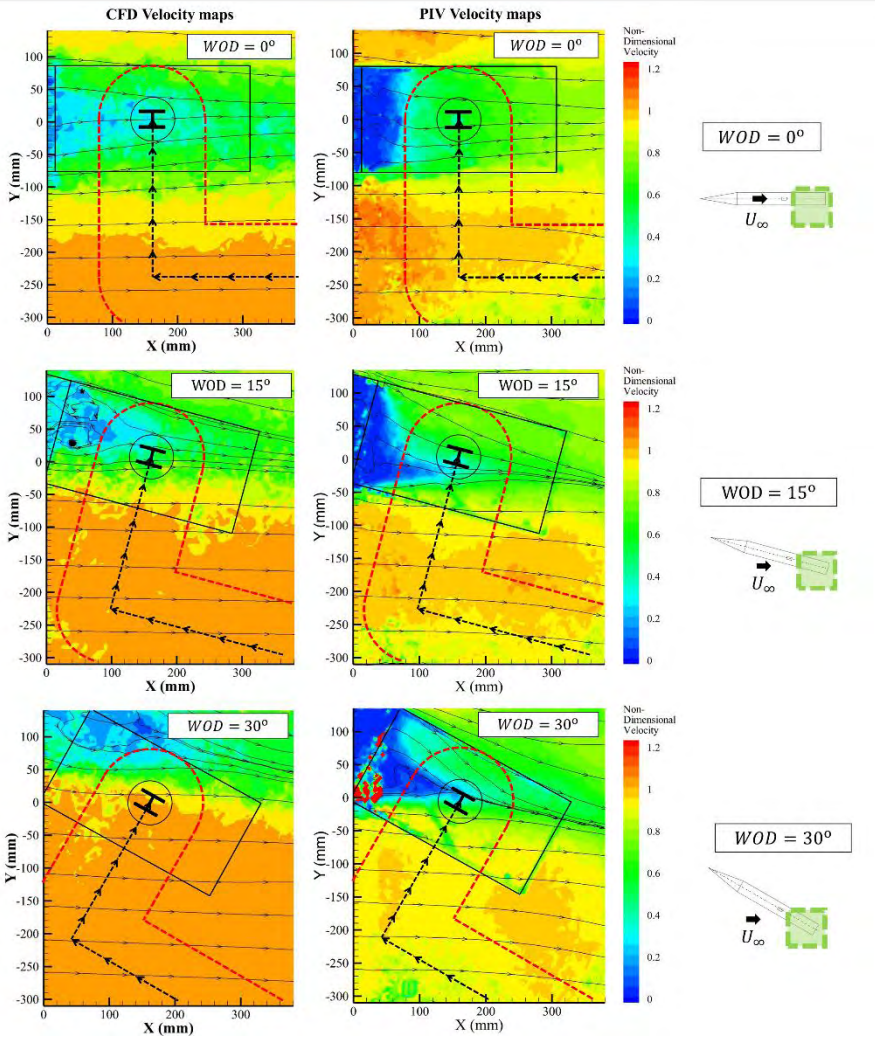

Figure 10: Interpolated CFD (left) and PIV non-dimensional velocity maps (right) at 0º and 15º and 30º.

For a more detailed comparison, a new set of maps has been obtained in *figures 11 to 13*. They represent the magnitude differences (ϵ) between experimental PIV and numerical maps,

$$\epsilon\ (\%) = |V_{PIV} - V_{CFD}| \times 100 \qquad (1)$$

In each of the following figures, the helicopter trajectory is represented again with black arrowed lines. The helicopter incident non-dimensional velocity profiles during these paths are plotted for the experimental (PIV) and numerical (CFD) results. The magnitude of relative differences (ϵ) between them are also plotted. Some important points are marked with letters to

match the helicopter position on the map and graphs (A, B, C, D). The helicopter position plotted in the graphs is the distance travelled by the helicopter when it follows the black arrowed lines.

Figure 11 represents the magnitude difference maps for WOD = 0º case. Map and plots show that the differences between experimental and numerical results are not so high in this case. Also, the incident velocities to the helicopter during the approach follow the same tendency. However, in the last phase of the maneuver (points B, C and D), the numerical results are always under the experimental, with maximal differences in magnitude of 20 and 30 %.

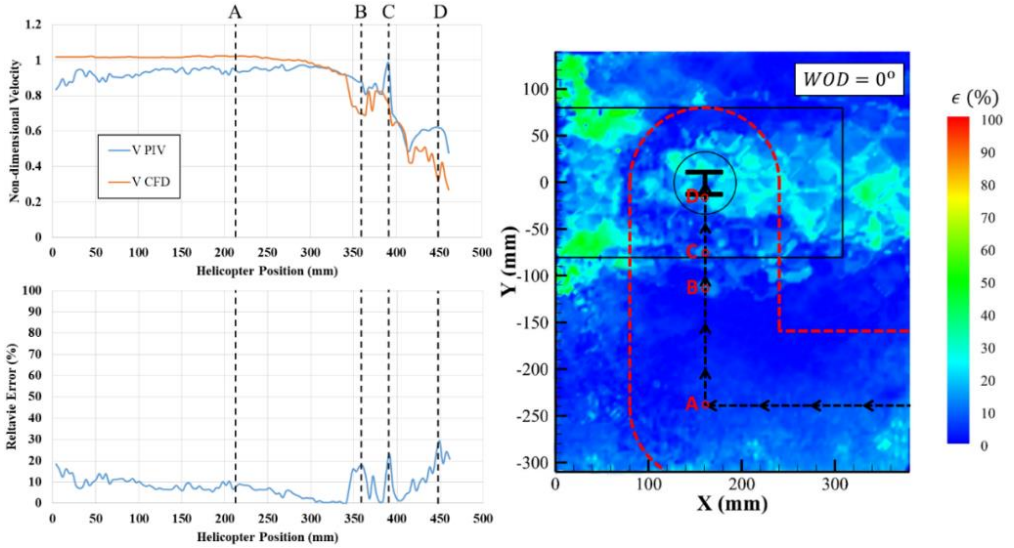

Figure 11: Magnitude difference maps for WOD = 0º. Plot of helicopter incident velocity during landing approach and magnitude difference between PIV and CFD.

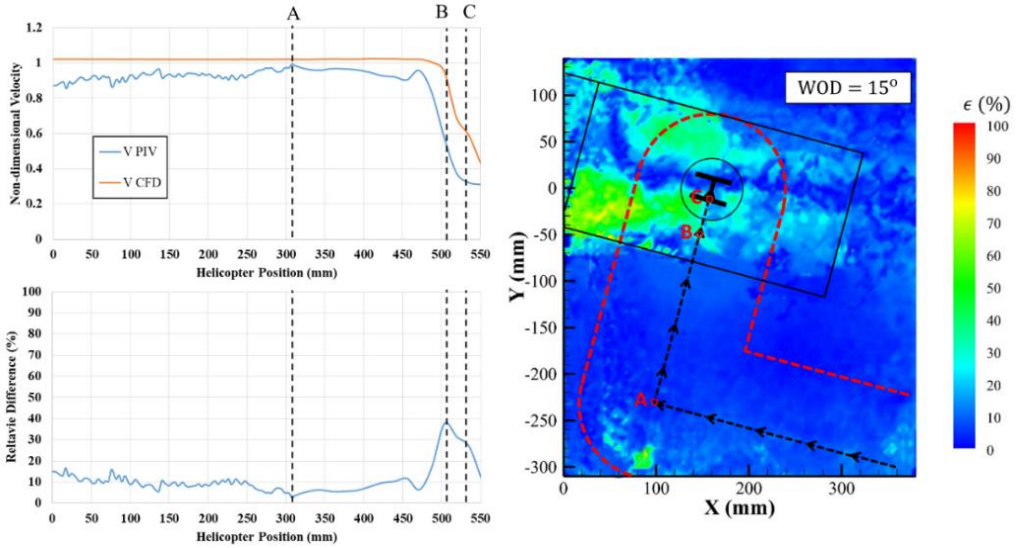

Figure 12: Helicopter incident velocity during landing approach. Interpolated CFD and PIV relative error for WOD = 15º.

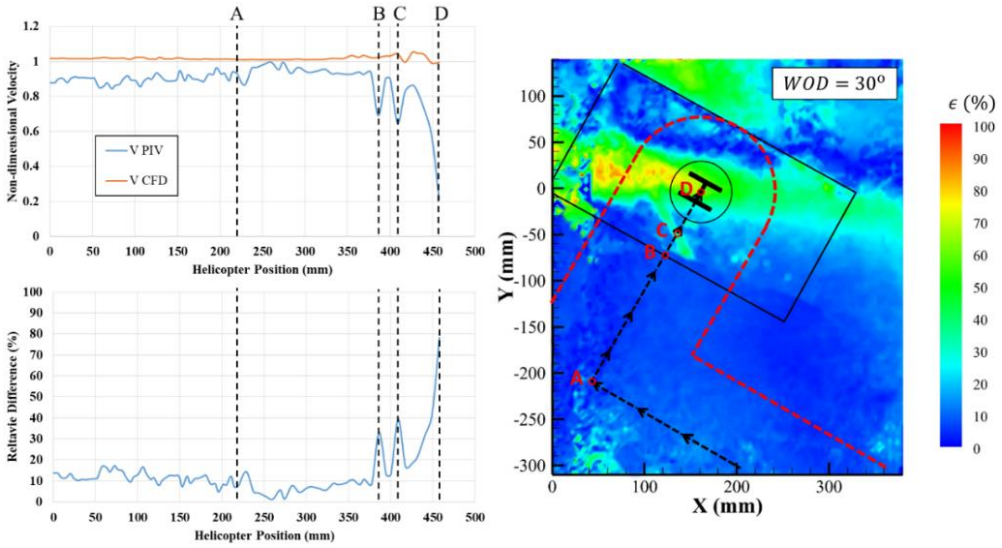

Figure 13: Helicopter incident velocity during landing approach. Interpolated CFD and PIV relative error for WOD = 30º.

Figure 12 represents the magnitude difference maps for WOD = 15º case. Map and plots show a similar tendency for the numerical and experimental results. However, higher relative differences are observed (up to 40 %). Contrary to the previous case, in the last phase of the maneuver, the numerical results show a higher value of incident wind velocity than the experimental results. This is because the numerical simulation predicts a recirculation bubble in an area above the final descending point (C), see *figure 10, CFD map* ($WOD = 15^o$).

Figure 13 shows the magnitude difference maps for $WOD = 30^o$ case. In this case, the relative differences were higher between experimental and numerical results. The reason for this may be that the recirculation bubble in the numerical results is predicted in a far zone from the helicopter descent point (D), see *figure 10 CFD map* ($WOD = 30^o$). And experimental results obtained from PIV technique show a recirculation bubble near from this point and a huge descent in incident velocities is produced for the helicopter, as seen in the non-dimensional PIV velocity profiles in *figure 15*.

6. CONCLUSIONS

Both numerical and PIV velocity maps obtained have shown that the helicopter landing approach on frigates is a very complex maneuver for pilots. This is due to the great change in its incident velocities and the turbulence intensity during its lateral approach to the contact point experienced by the helicopter rotor. And it is worse when the incident wind angle increases.

In general, the comparison between numerical and experimental results obtained on the rotor plane above the helicopter aft-deck have shown a great resemblance. This means that the streamlines, velocity magnitude and main flow patterns of the maps obtained experimentally (PIV) and numerically (CFD) are very similar. However, in a more detailed comparison, when the incident velocities during the path of the helicopter approach are compared, differences are more significant (up to 40 % at certain points). In addition, differences between numerical and experimental results become higher with the increment of wind over deck angle. This difference could be due to the fact that numerical simulation predicts a smaller recirculation bubble behind the superstructure. Another reason is that the numerical results show always this bubble aligned

with the incident wind velocity and its direction does not change significantly with the change in WOD (Wind Over Deck) angle.

All data presented in this paper could be a very useful basis for future comparatives and validation of numerical results obtained by Computational Fluid Dynamics codes (CFD). This is because a standardized and simplified frigate shape (SFS2), which is easy to study numerically due to its geometry, has been used. In addition, the simple interpolation process followed to compare experimental PIV data and numerical, could be useful to enable effective collaboration between both ways of dealing with the aerodynamic problem on frigates. Numerical tests could help the process to save time and money avoiding expensive long wind-tunnel testing campaigns. Experimental tests could do the same providing results that help to improve turbulence models and the accuracy of numerical results.

Finally, it has been shown that is very important to carry out wind tunnel tests and numerical predictions to certify and establish operational limits related to helicopters maneuvers on frigates. It should also be noted that any new frigate should be tested in this way to detect possible aerodynamic peculiarities caused by its superstructure geometry and thus correctly determine the flight envelopes of aircraft maneuvers on its deck. In the future, these tests and its results will increase the safety of helicopter operations on frigates.

REFERENCES

[1] Kääriä, C. Wang Y., White M. and Owen I. An experimental technique for evaluating the aerodynamic impact of ship superstructures on helicopter operations", *Ocean Engineering*, vol. 61, pp. 97-108, 2013. Elsevier Publishing.

[2] Swales, C. and Breeze, G. LDV measurements above the flight deck of a model frigate. In: 35th aerospace sciences meeting & exhibit, Reno, NV, 6-9 January 1997. Reston, VA: AIAA.

[3] Wakefield, N. Newman S. and Wilson P., Helicopter flight around a ship's' superstructure. *Proceedings of the Institution of Mechanical Engineers, Part G: Journal of Aerospace Engineering*, vol. 216, no. 1, pp. 13-28, 2002.

[4] Kääriä, C. Investigating the impact of ship superstructure aerodynamics on maritime helicopter operations. PhD Thesis, School of Engineering, University of Liverpool, UK, 2012

[5] Lumsden, R. B. Ship air-wake measurement, prediction, modelling and mitigation *Defence Science and Technology Laboratory, UK*, 2003.

[6] Rajasekaran, J. On the flow characteristics behind a backward-facing step and the design of a new axisymmetric model for their study. *Doctoral dissertation, University of Toronto*, 2011.

[7] Nacakli, Y. Landman, D. and Doane, S. Investigation of Backward-Facing-Step Flow Field for Dynamic Interface Application, *Journal of the American Helicopter Society*, vol. 57, no. 3, pp. 1-9, 2012.

[8] Shafer, D.M. Ghee, T.A. Active and passive flow control over the flight deck of small naval vessels. 35th AIAA Fluid Dynamics conference and Exhibit, Fluid Dynamics and Co-

located Conferences, Toronto, Ontario, Canada, 2005.

[9] Bardera-Mora, R. Barcala-Montejano, M. Rodríguez-Sevillano, A. de Diego, G. and de Sotto, M. A spectral analysis of laser Doppler anemometry turbulent flow measurements in a ship air wake, *Proceedings of the Institution of Mechanical Engineers, Part G: Journal of Aerospace Engineering*, vol. 229, no. 12, pp. 2309-2320, 2015.

[10] Brownell, C. Luznik, L. Snyder, M. Kang, H. and Wilkinson, C. In Situ Velocity Measurements in the Near-Wake of a Ship Superstructure, *Journal of Aircraft*, vol. 49, no. 5, pp. 1440-1450, 2012.

[11] Lee, R. and Zan, S. "Wind tunnel testing to determine unsteady loads on a helicopter fuselage in a ship airwake". In *ICAS 2002 Congress* (pp. 3111-1), 2002.

[12] Lee, R. and Zan, S. Wind Tunnel Testing of a Helicopter Fuselage and Rotor in a Ship Airwake. *Journal of the American Helicopter Society*, vol. 50, no. 4, pp. 326-337, 2005.

[13] Doane, S. R. and Landman, D. A. A wind tunnel investigation of ship airwake/rotor downwash coupling using design of experiments methologies. In *Proceedings of the 50th AIAA Aerospace Sciences Meeting including the New Horizons Forum and Aerospace Exposition* (pp. 2012-0767), 2012.

[14] Foeken, M. Pavel, M. D. Investigation on the simulation of helicopter/ship operations. Faculty of Aerospace Engineering, Delft University of Technology Kluyverweg 1, 2629 HS, Delft, The Netherlands.

[15] Yuan, W., Wall, A. and Lee, R. Combined numerical and experimental simulations of unsteady ship airwakes, *Computers & Fluids*, vol. 172, pp. 29-53, 2018.

[16] Yuan W., Lee R., Wall A., "Simulation of Unsteady Ship Airwakes Using Openfoam". 30th Congress of the International Council of the Aeronautical Sciences. DCC, Daejeon, Korea: September 25-30, 2016.

[17] Mora, R. "Experimental Investigation of the Flow on a Simple Frigate Shape (SFS)", *The Scientific World Journal*, vol. 2014, pp. 1-8, 2014.

[18] White, F. *Fluid Mechanics*, 4th Edition. McGraw Hill Companies, 2002, pp. 298-299.

[19] Raffel, M. Willert, C. Scarano, F. Kähler, C. Wereley, S. and Kompenhans, J. *Particle Image Velocimetry*. Springer, 2007.

[20] Adrian, R. and Westerweel, J. *Particle Image Velocimetry*. Cambridge: Cambridge University Press, 2011.

[21] Prasad, A. K. *Particle Image Velocimetry*. Curr Sci 2000; 79(1): 10

[22] Adrian, R. Particle-Imaging Techniques For Experimental Fluid-Mechanics, *Annual Review of Fluid Mechanics*, vol. 23, no. 1, pp. 261-304, 1991.

[23] Kähler, C. Sammler, B. and Kompenhans, J. Generation and control of tracer particles for optical flow investigations in air, *Experiments in Fluids*, vol. 33, no. 6, pp. 736-742, 2002.

[24] Echols, W. H. and Young, J. A. Studies of portable air-operated aerosol generators (No. NRL-5929). NAVAL RESEARCH LAB WASHINGTON DC, 1963.